LRP 511/95 March 1995

LOW POWER EXCITATION OF GYROTRON-TYPE MODES IN CYLINDRICAL WAVEGUIDE USING QUASI-OPTICAL TECHNIQUES

N.L. Alexandrov, G.G. Denisov, D.R. Whaley & M.Q. Tran

submitted for publication to
Int. J. of Electronics

Low power excitation of gyrotron-type modes in cylindrical waveguide using quasi-optical techniques

N. L. Alexandrov‡, G. G. Denisov*, D. R. Whaley†, M. Q. Tran†

‡Centre de Recherches en Physique des Plasmas, Ecole Polytechnique Fédérale de Lausanne, Association Euratom-Confédération Suisse, 21 Av. des Bains, CH-1007 Lausanne, Switzerland
Permanent address: Institute of Applied Physics, Russian Academy of Science, 46, Uljanov Street, 603600 Nizhny Novgorod, Russia

*Institute of Applied Physics, Russian Academy of Science, 46, Uljanov Street, 603600 Nizhny Novgorod, Russia

†Centre de Recherches en Physique des Plasmas, Association Euratom-Confédération Suisse, Ecole Polytechnique Fédérale de Lausanne, 21 Av. des Bains, CH-1007 Lausanne, Switzerland

Abstract

Experimental results of low power excitation of a *118 GHz* $TE_{22,6}$ rotating mode are presented. A rectangular waveguide mode is converted to a $TE_{22,6}$ circular waveguide mode using quasi-optical techniques. A good conversion efficiency is measured and the experimentally observed field intensity profiles show the percentage of unwanted modes to be small.

1. Introduction

High-order gyrotron-type modes have a complex electric field spatial structure.. In a gyrotron, such a structure can be transformed into a linearly polarized, narrowly directed free-space beam using different types of converters (Vlasov *et al.* 1975, Möbius *et al.* 1991, Denisov *et al.* 1992). Using a high-order mode source, it becomes possible to verify the design of these converters before installation into the gyrotron. For this reason, the *118 GHz* $TE_{22,6}$ source described in this paper was designed, constructed and tested. There are different methods to produce high-order circular waveguide modes (Hea *et al.* 1993, Aleksandrov *et al.* 1992, Moeller 1992, Thumm *et al.* 1990, Thumm *et al.* 1988). The design of this source uses the method described by Aleksandrov *et al.* (1992) - quasi-optical excitation of a translucent-wall cylindrical cavity. For such a method, problems with mode competition are common. If modes exist with similar spatial structure to the desired mode and with a resonant frequency near to that of the desired mode, excitation of these nearby modes can occur. In the case of excitation of the $TE_{22,6}$ mode in a hollow cylindrical waveguide, the $TE_{25,5}$ mode is such a competitor with $(\nu_{22,6}-\nu_{25,5})/\nu_{22,6} = 1.4 \times 10^{-3}$ where $\nu_{m,n}$ is the eigenvalue of mode TE_{mn}. To

"separate" these modes one can design a cavity with a sufficiently high quality factor, e.g. for $Q = 11000$ the spectral overlap is ~0.1%. However in practice, cavities with low quality factors are more acceptable, providing a good conversion efficiency and eliminating the problem of required source stability. To allow for this as well as provide good mode purity with nearby modes well separated from the desired mode in the mode spectrum, a coaxial cavity (Goldenberg *et al.* 1993) is used.

The $TE_{22,6}$ converter using a coaxial cavity was constructed and tested and the results are reported here. A general overview of the converter as well as a discussion of the quasi-optical components are presented in §2. The coaxial cavity is discussed in §3. Experimental results including measured radiation wave field profiles are presented in §4. Concluding remarks are presented in §5.

2. $TE_{22,6}$ mode converter - quasi-optical component design.

The $TE_{22,6}$ mode converter was designed using the results presented by Aleksandrov *et al.* (1992) and a drawing of the converter is shown in Fig. 1. The converter is comprised of a corrugated Gaussian horn, two microwave mirrors, coaxial cavity and a fixing structure shown in the figure.

The shapes for both mirrors are computed using geometrical optics. A Gaussian horn with a large divergence is used ($k_0 w_0 = 6$ where k_0 is the free space wave number and w_0 is the waist, $1/e$ in power, of the Gaussian beam generated by the horn). The first mirror is designed such that the horn lies at the mirror's first focus. The second focus, in the horizontal direction, lies at a distance equal to the sum of the distances between the first and second mirrors and between the second mirror and the $TE_{22,6}$ caustic in the resonant cavity. The central ray is used to determine these distances. In the vertical direction, the first mirror transforms all rays into parallel rays. As a result the surface of mirror number one has the following form:

$$z' = B\sqrt{1 - 2\left(\frac{x'}{2B}\right)^2 - \left[\frac{y'}{A} + \left(\frac{x'}{2B}\right)^2 \frac{F}{A}\right]^2 + \left(\frac{x'}{2B}\right)^4} \qquad (1)$$

where $F = \sqrt{A^2 - B^2}$, $A = (R_1 + R_2) / 2$, and $B = \sqrt{R_1 R_2}\cos\beta$. Here R_1 and R_2 are the input and output focal lengths of the mirror, and β is the incident angle. The coordinate system is as shown in Fig. 1 and Eq. 1 refers to the insert with the primed coordinate system. This system is rotated by 20.23° around the x axis relative to the unprimed coordinate system. The direction of polarization of the incident Gaussian beam and the direction of rotation of the output $TE_{22,6}$ mode are shown. For the remainder of

this paper, the mode with the correct direction of rotation, as defined in Fig. 1, will have the notation $TE_{22,6}$ or $TE^{+}_{22,6}$ and the mode with the opposite direction of rotation will have the notation $TE^{-}_{22,6}$.

The second mirror is a quasi-parabolic mirror (Vlasov *et al.* 1975) similar to those used in gyrotrons which employ a quasi-optical system to convert high-order waveguide modes to a free-space Gaussian mode. In this case the mirror operates in a reverse sense - converting a beam with parallel rays into a beam with a caustic of that of the $TE_{22,6}$ cavity mode. The mirror is positioned such that the beam illuminates the translucent wall of the cavity and the caustic lies inside the cavity at the same location as that of the corresponding $TE_{22,6}$ cavity field. The frequency is then chosen as that of the $TE_{22,6}$ resonant cavity frequency and the $TE_{22,6}$ mode is excited.

3. $TE_{22,6}$ mode converter - coaxial cavity design.

A schematic of the coaxial cavity is shown in Fig. 2 and is comprised of a tapered circular waveguide with the central rod and a smooth up-taper. The coaxial cavity is used to decrease competition between the $TE_{22,6}$ mode and nearby modes in the mode spectrum. The eigenvalues for coaxial waveguide are plotted in Figs. 3 as a function of the radius ratio c where $c = a/b$ with a = outer radius of the cylindrical section of the cavity and b = inner radius of the cylindrical section of the cavity. The behavior of the eigenvalues as a function of c is different for different modes. As a result, with a coaxial cavity the $TE_{22,6}$ can be separated in frequency from its nearest competitor, the $TE_{25,5}$ mode. The cavity is built with a radius ratio of $c = 2.23$. As shown in Figs. 3, this allows for the best separation of modes with similar frequency and spatial structure (e.g. $TE_{25,5}$, $TE_{32,3}$, $TE_{19,7}$). Modes with azimuthal indices $m << 22$, which also exist near the chosen eigenvalue, are much less dangerous for modes competition as the behavior of the "rays" in a cavity in the geometrical approximation is much different for modes with largely different azimuthal indices. The choice of $c = 2.23$ is also chosen because at this value of c the $TE_{22,6}$ eigenvalue is a slowly varying function of c. Machining errors then do not strongly affect the cavity characteristics - resonant frequency and quality factor. And lastly, the field structure at this value of c is not greatly different that that of a hollow cavity as shown in Figs. 4(a) and (b). This would not be the case with smaller values of c. After the resonant section of the cavity, the outer wall and inner rod are tapered to a value of $c = 3.5$. At this value of c, the rod does not affect the $TE_{22,6}$ waveguide field, shown in Fig. 4(c), and the rod is abruptly terminated. The outer wall is then connected to a standard circular waveguide which transports the generated $TE_{22,6}$ mode to the quasi-optical system to be tested.

To provide the cavity coupling, part of the wall of the cavity is made translucent to the illuminating microwave beam. The wall, with a thickness of $\sim 0.5mm$, is made translucent with a grid of radially drilled holes of $0.8mm$ diameter. A schematic of the holes is shown in Fig. 5. The azimuthal extent of the grid is $110°$ and the azimuthal spacing of the holes is chosen so as not to lie on the peaks of a $TE_{22,6}$ cavity standing wave. The axial spacing as well as the diameter of the holes and the thickness of the wall are chosen as a compromise of the requirements to provide reasonably good coupling, to maintain the resonance properties of the cavity, and to avoid manufacturing difficulties. The grid is $31mm$ in length and contains 506 coupling holes, 22 axially × 23 azimuthally.

The cavity is designed for a frequency of $f = 118\ GHz$. The calculation of the frequency is based on that of a hollow cavity. A program integrating the wave equation along the cavity, imposing a cutoff condition at the input of the cavity and a traveling wave condition at the output of the cavity computes the cold cavity diffraction quality factor Q_{diff} and resonant frequency. The dimensions of the equivalent hollow cavity are determined as those which give a resonant frequency of 118GHz × (ν(hollow cavity)/ν(coaxial cavity).

The quality factor of any resonator is defined as:

$$Q = \frac{\omega W}{P_{loss}} \tag{2}$$

where ω is frequency, W is the stored energy of the mode and P_{loss} is the power loss of the cavity. Since the field structure for a coaxial cavity of $c = 2.23$ is similar to that of a hollow cavity, the ohmic quality factor is estimated with Eq. 2 using the field expressions for a hollow cavity to estimate W. The losses on the outer wall and on the central rod are, however, computed using the actual coaxial fields. The result for the ohmic quality factor, Q_{ohm}, is:

$$Q_{ohm} \approx \frac{a}{d} \frac{\left(1 - \left(m / \nu_{mn}\right)^2\right)}{1 + \frac{b}{a} \frac{Z_m^2(k_\perp b)}{Z_m^2(k_\perp a)}} \tag{3}$$

where $$Z_m(\nu_{mn} \frac{r}{a}) = J_m(\nu_{mn} \frac{r}{a}) Y_m'(\nu_{mn} / c) - Y_m(\nu_{mn} \frac{r}{a}) J_m'(\nu_{mn} / c)$$

and $k_\perp = \nu_{mn}/a$, $J_m(x)$ is the J Bessel function of order m, $Y_m(x)$ is the Y Bessel function of order m, d is the skin depth, ($d = 5.1 \times 10^{-7}\ m$ for non-ideal brass at $f = 118\ GHz$ with $\sigma = 8.5 \times 10^6\ \Omega^{-1} m^{-1}$). Therefore

$$Q_{ohm} \approx 1.4 \times 10^4. \tag{4}$$

As stated above, the diffractive quality factor is computed numerically. For the chosen cavity, Q_{diff} is computed to be:

$$Q_{diff} \approx 4.0 \times 10^3. \tag{5}$$

The grid quality factor can be calculated using Eq. 2. This factor represents the losses due to the power radiated through the grid of holes in the wall of the cavity. Assuming, that the transparency of the wall is low, the following expression is obtained:

$$Q_{grid} = \frac{2\pi}{\Theta} \frac{\nu_{mn}\left(1 - \left(m / \nu_{mn}\right)^2\right)}{T^2} \tag{6}$$

where 2Θ is the azimuthal extent of the translucent area in radians, T^2 is the transmission coefficient of the wall in power. This coefficient can be estimated for a plane surface with the same parameters as those of the wall of the cavity using the method of Westermann *et al.* (1964). Using an effective thickness of the wall of $t = 0.3mm$ the transmission coefficient is computed as: $T^2 = 6 \times 10^{-3}$ and the grid quality factor becomes:

$$Q_{grid} \approx 5.0 \times 10^4. \tag{7}$$

With the above estimates of Q_{diff}, Q_{ohm}, and Q_{grid}, the total quality factor can be calculated to be:

$$Q_{tot} \approx 2.9 \times 10^3. \tag{8}$$

This value is to be compared to the measured total quality factor of §4.

One can attempt to maximize the output power by varying the value of Q_{grid}. Since $P_{output} \propto Q_{tot}^2 / (Q_{grid} Q_{diff})$, one can show that the maximum output power occurs at $1/Q_{grid} = 1/Q_{ohm} + 1/Q_{diff}$. To fulfill this condition the present value of Q_{grid} should decrease. One may decrease Q_{grid} by increasing the coupling hole diameter or by decreasing the wall thickness. Increasing the hole diameter, however, increases the risk of mode mixing because this compromises the effective surface quality of the cavity and reradiation of the resonance mode power in non-resonant modes can occur. Large holes also decrease the resonance properties of the cavity. A wall thickness of $t = 0.5\ mm$ is a reasonable value when considering ease of machining and final wall rigidity. With the above expression for P_{output}, one also sees that the coupling power is relatively

insensitive to the value of Q_{grid}. Therefore the above considerations on hole size and wall thickness are used instead of considerations of maximum coupling to determine the values used in the construction of the cavity.

4. Experimental results.

The RF power for the low power tests is generated by a TH4215 carcinotron with a frequency range of $115\ GHz < f < 150\ GHz$ and an output power of $\sim 0.5\ W$. The RF power near $f = 118\ GHz$ propagates through D-band waveguide to the input Gaussian horn of the converter. The output waveguide of the coaxial cavity is of diameter $\varnothing 40mm$ and an additional uptaper to $\varnothing 48mm$ was used for the measurements. The waveguide field is measured at the output of this additional uptaper. The field measurement is made with a diode detector followed by an amplifier and data acquisition system. The detector is mounted on a moveable programmable xy table with typically 10000 measurements taken for each $TE_{22,6}$ field pattern. The dynamic range of the measurement system is $\sim 33dB$.

The experimental results of the low-power tests are presented in Figs. 6-9. In addition to field measurements at the output of the converter, measurements of the field distribution at the intermediate mirror positions are shown. Figure 6 shows the field distribution at the location of the first mirror measured on a plane perpendicular to the axis of the Gaussian horn. Figure 7 then shows the transformed beam at the location of the second mirror measured in a plane perpendicular to the line connecting the center of the two mirrors.

The output of the second mirror illuminates the grid of holes in the cavity wall and the frequency is varied to match the $TE_{22,6}$ resonant frequency. Several central cavity rods of slightly different diameters were made to be able to vary the eigenvalue of the $TE_{22,6}$ mode and the corresponding frequency. The first measurement showed a resonant frequency at $f = 117.95\ GHz$. This shift in the resonance frequency from $118\ GHz$ can be explained by a machining error in the diameter of the cavity of $0.02mm$. The central rod was then replaced with one of slightly smaller diameter, changed from $16.44\ mm$ to $16.34\ mm$ and the resonant frequency increases to $118.06\ GHz$. All measurements were made at this frequency.

The resonance curve of the $TE_{22,6}$ mode for the experimental setup just described is shown in Fig. 8. A best fit to the data points with a theoretical resonance curve shows the resonance frequency of $f = 118.06\ GHz$ and $Q_{tot} \sim 2800$. This value is to be

compared to the calculated Q_{tot} value from §3 of $Q_{tot} \sim 2900$. These values are in excellent agreement.

The $TE_{22,6}$ field profile measured at the output of the cavity is shown in Fig. 9a. This is a measurement of $|E_y|^2$ and is to be compared with the theoretical $|E_y|^2$ field pattern shown in Fig. 9(b). The agreement is seen to be excellent. With such cavities, the problem of mixing of the $TE_{22,6}$ mode of the counter rotation must be considered. The cavity was optimized experimentally to minimize the mix of the $TE^{-}_{22,6}$ mode. The content of the counter-rotating mode in the output signal can be estimated by measuring the minimum-to-maximum voltage ratio of the modulation of the signal in azimuth due to interference of the two rotating modes. Here, a voltage measurement is assumed to be proportional to incident power. The content of the counter-rotating mode as a function of this voltage ratio is shown in Fig. 10 and for a typical output beam from the converter the standing wave ratio is 0.8 corresponding to a mode mix of $P^{-}_{22,6} \; / \; P^{+}_{22,6} \sim 0.3\%$. The excitation of modes near in the spectrum to the $TE_{22,6}$ mode, $TE_{0,9}$, $TE_{1,9}$, etc., was seen to be sensitive to the position of the center rod. The final experimental setup was also optimized to minimize the content of these modes and from Fig. 9(a) it is seen that the mode mixture with these modes is small. The electric field in the center of the waveguide is measured to be more than $23dB$ below the peak value at $r/a \sim 0.5$.

The conversion efficiency of this converter is estimated by the following:

$$\eta_{conv} = \frac{P_{output}}{P_{input}} \approx \frac{k_{//}}{k_0} \frac{a^2}{w_x w_y} \left(1 - \frac{m^2}{\nu_{mn}^2} \right) \frac{J_m^2(\nu_{mn})}{J_m^2(m)} \frac{U_{output}}{U_{input}} \tag{9}$$

where $k_{//} = \sqrt{k_0^2 - k_\perp^2}$, U_{output} is the signal measured on the caustic of the output mode, U_{input} is the signal measured at the center of the Gaussian input beam, and $w_{x,y}$ is the spot size in the x, y direction at the location where U_{input} is measured. U_{input} and U_{output} are assumed to be signals whose values are proportional to incident power. Above, it is assumed that $r_c \sim m/k_\perp$ where r_c is the caustic radius of the output beam. These low power measurements give:

$$\eta_{conv} \approx 0.13 \tag{10}$$

which is a good conversion efficiency for such types of converters.

5. Conclusions.

The design and tests of a low power $TE_{22,6}$ mode converter have been presented. The design equations for the quasi-optical system are shown that convert the input

Gaussian microwave beam to a beam which will excite the $TE_{22,6}$ mode in the given coaxial cavity. The coaxial cavity design is shown to separate the $TE_{22,6}$ mode from nearby competing modes. A cavity hole grid design is presented which is a good compromise between wall translucency, machining ease, and structural rigidity. The total quality factor is measured and seen to be in good agreement with calculation. The mode mix in the final output beam is measured to be small and the conversion efficiency is seen to be good. This converter is presently being successfully used to perform low power verification of the quasi-optical system design for a *118 GHz* $TE_{22,6}$ gyrotron.

ACKNOWLEDGMENTS

The authors would like to thank J.-C. Magnin and W. Matthey-Doret at the CRPP for help in fabrication of many components of the converter. One of the authors, N. Alexandrov, was supported by the Branco Weiss Fellowship of the Swiss Academy of Engineering Sciences.

REFERENCES

Aleksandrov, N., Chircov, A., Denisov, G., Vinogradov, D., Kasparek, W., Pretterebner, J., and Wagner, D., "Selective excitation of high-order modes in circular waveguides", *Int. J. Infrared and Millimeter Waves*, **13**, No. 9, 1992.

Denisov, G. G., Kuftin A. N., Malygin, V. I., Venediktov, N. P., Vinogradov, D. V., and Zapevalov, V. E., "110GHz gyrotron with a built-in high efficiency converter", *Int. J. Electronics*, **72** 1079 1992.

Goldenberg, A. L., Khizhnyak, V. I., Pavelyev, A. B., Pylin, A. V., "Perspectives of coaxial cavity applications in powerful long-pulse gyrotrons of mm wavelength range", *Proc. 2nd International Workshop on Strong Microwaves in Plasmas*, Nizhny Novgorod 1993.

Hea, T. A., Peebles, R. A., Vernon, R. J., "A traveling wave resonator for exciting whispering gallery modes in an overmoded circular waveguide", *Proc. 18th Int. Conf. Infrared and Millimeter Waves*, Colchester, October 1993.

Möbius, A., Pretterebner, J., "Avoidance of edge diffraction effects of WGM-fed quasi-optical antennas by feed waveguide deformation, *Proc. 16th Int. Conf. Infrared and Millimeter Waves*, Lausanne, August 1991.

Moeller, C., "A coupled cavity whispering gallery mode transducer", *Proc. 17th Int. Conf. Infrared and Millimeter Waves*, Pasadena, December 1992.

Vlasov, S., Zagryadskaya, L., and Petelin, M., *Radio Engineering and Electronic Physics*, **20** N10 1975.

Thumm, M., Jacobs, A., "In-waveguide TE_{01}-to-whispering gallery mode conversion using periodic wall perturbations", *Proc. 13th Int. Conf. Infrared and Millimeter Waves*, Honolulu, October 1988.

Thumm, M., Jacobs, A., Pretterebner, J., "Generation of rotating high order $TE_{m,n}$ modes for cold test measurements on high power quasi-optical gyrotron output mode converters", *Proc. 15th Int. Conf. Infrared and Millimeter Waves*, Orlando, December 1990.

Westermann, Z., and Maier, W., Zeitschrift Fuer Physik, 179 (I) 1964.

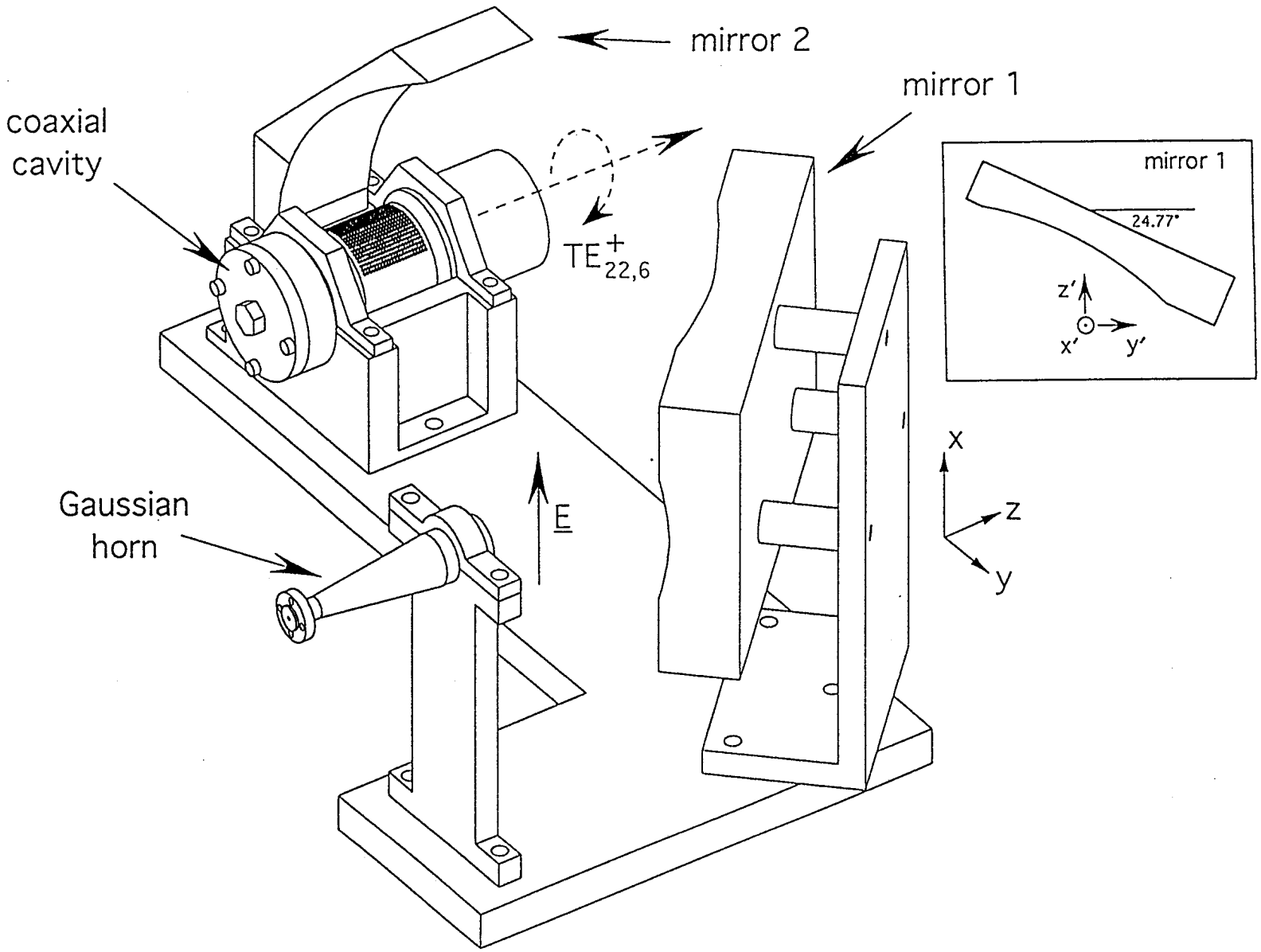

Figure 1. $TE_{22,6}$ mode converter. Shown is the Gaussian horn, two quasi-optical mirrors, coaxial cavity and support structure. The polarization of the input horn is shown as well as the desired rotation direction of the output $TE_{22,6}$ mode.

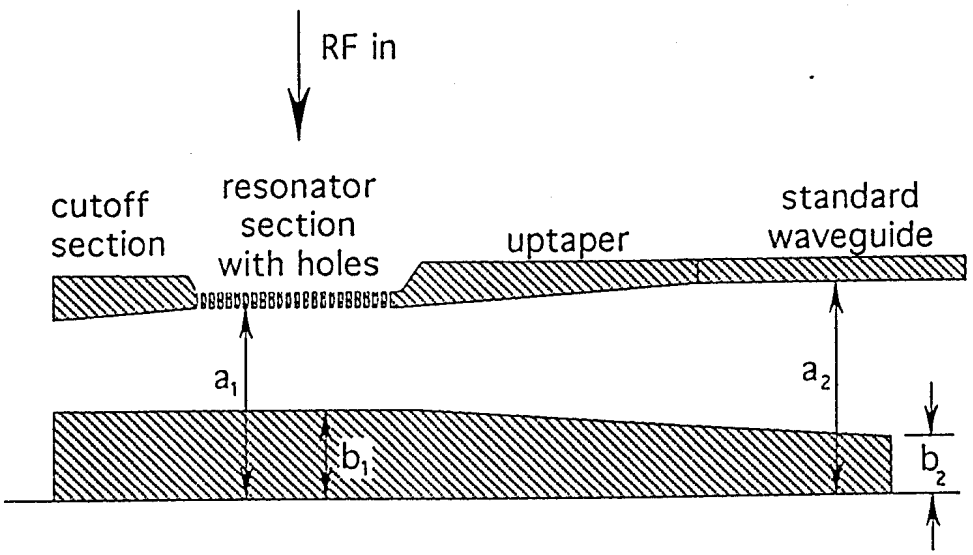

Figure 2. Schematic of coaxial cavity. The radius ratios shown are $c_1 = a_1/b_1 = 2.23$ and $c_2 = a_2/b_2 = 3.50$. The cutoff section and uptaper are designed with angles of $2°$.

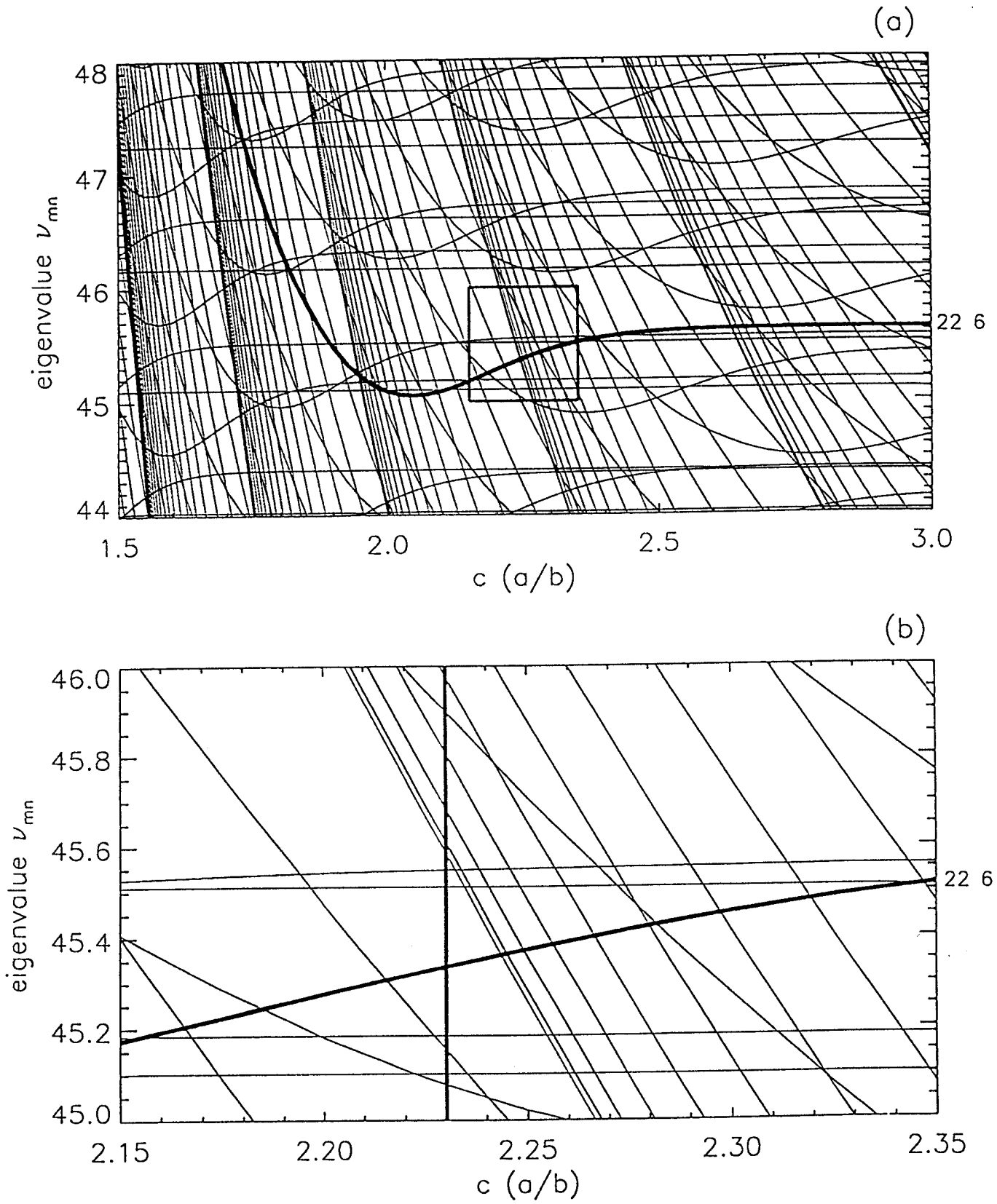

Figure 3. Eigenvalues in a coaxial cavity vs. radius ratio c. The bold square in (a) is expanded in (b) A choice of $c = 2.23$ gives a good separation from possible competing modes.

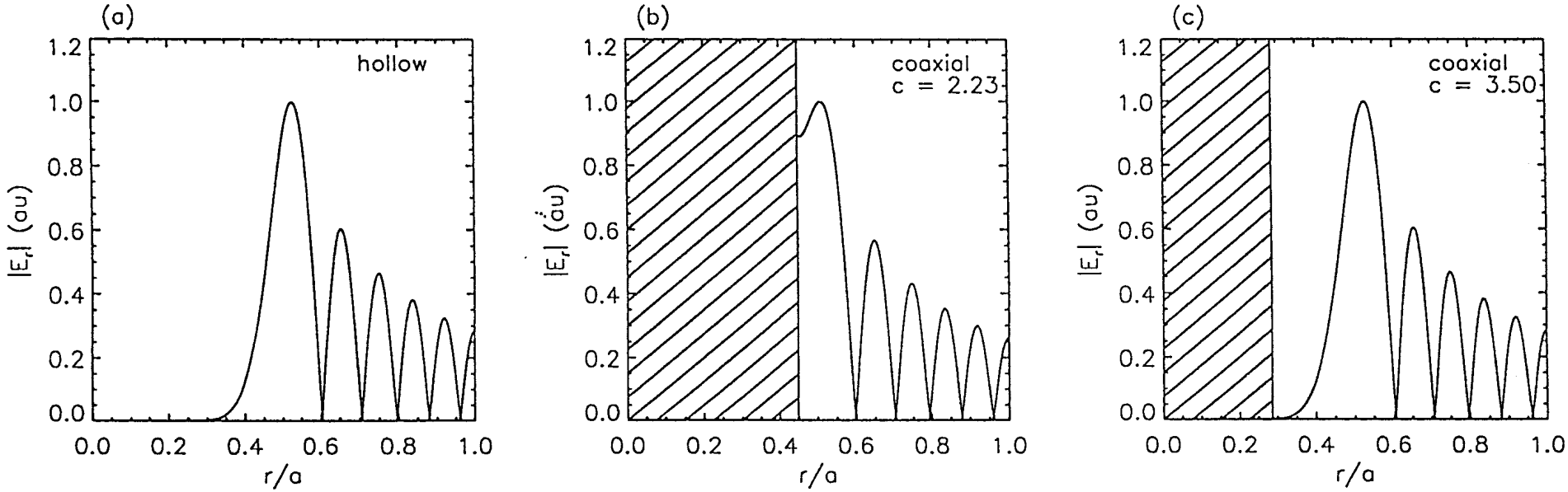

Figure 4. (a) $|E_r|$ for hollow cavity (b) $|E_r|$ for coaxial cavity with $c = 2.23$ - resonator section (c) $|E_r|$ for coaxial cavity with $c = 3.50$ - end of uptaper.

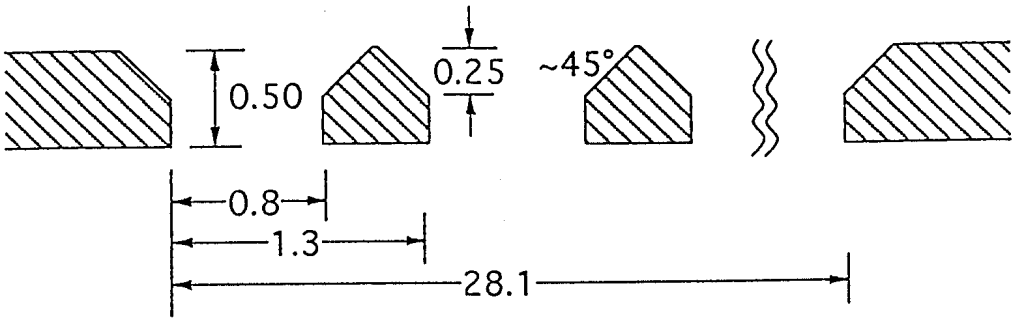

Figure 5. Schematic of holes in grid of coaxial cavity wall. The grid consists of a total of *22* holes axially × *23* holes azimuthally. The azimuthal extent of the grid is *110°*. All dimensions are in mm.

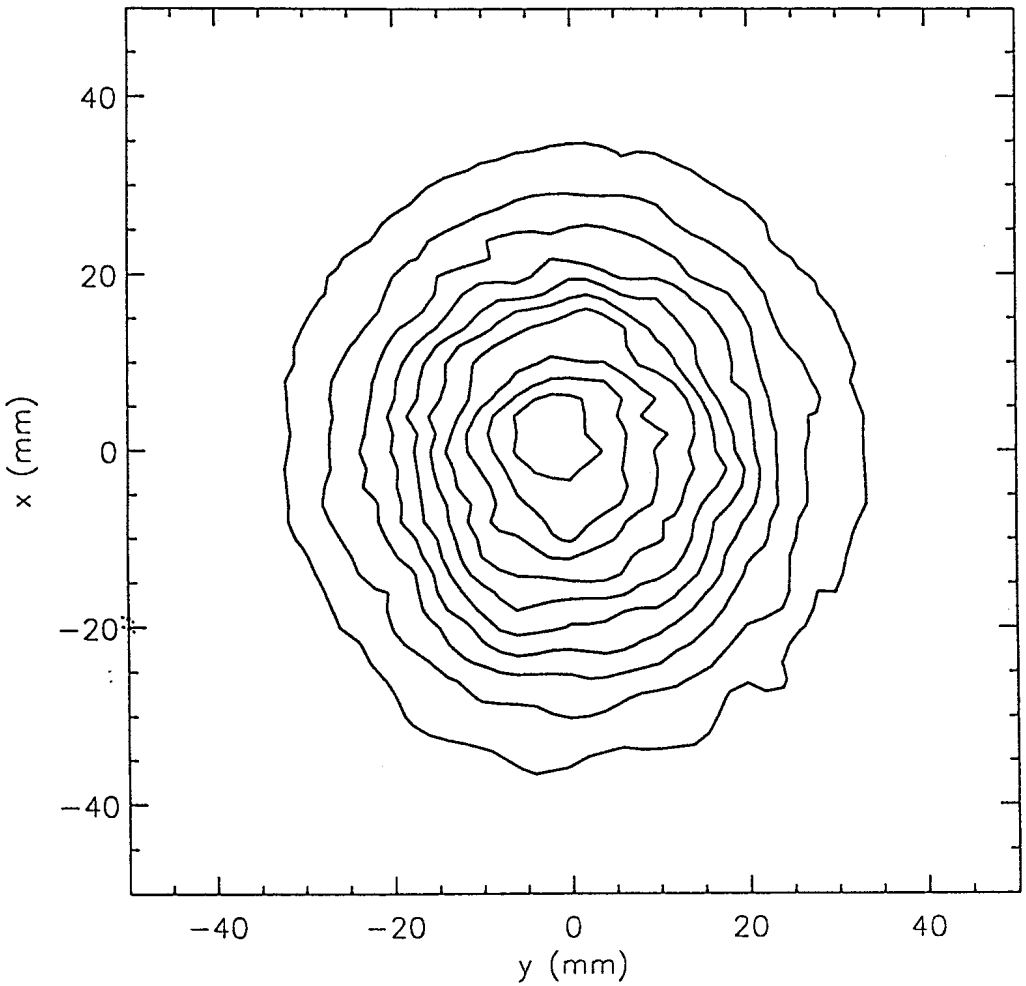

Figure 6. $|E_x|^2$ field distribution of the microwave beam at the location of the first mirror measured on a plane perpendicular to the axis of the Gaussian horn.

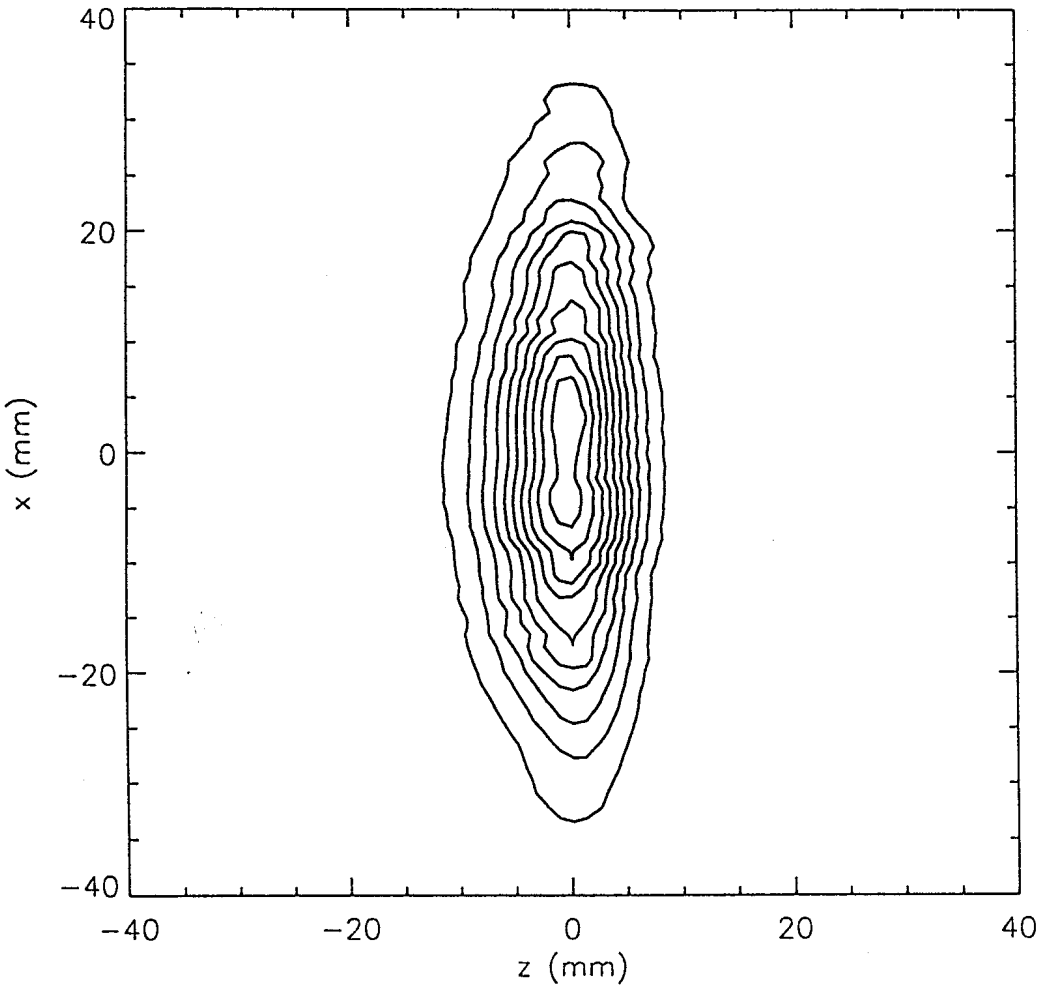

Figure 7. $|E_x|^2$ field distribution of the microwave beam at the location of the second mirror measured in a plane perpendicular to the line connecting the center of the two mirrors.

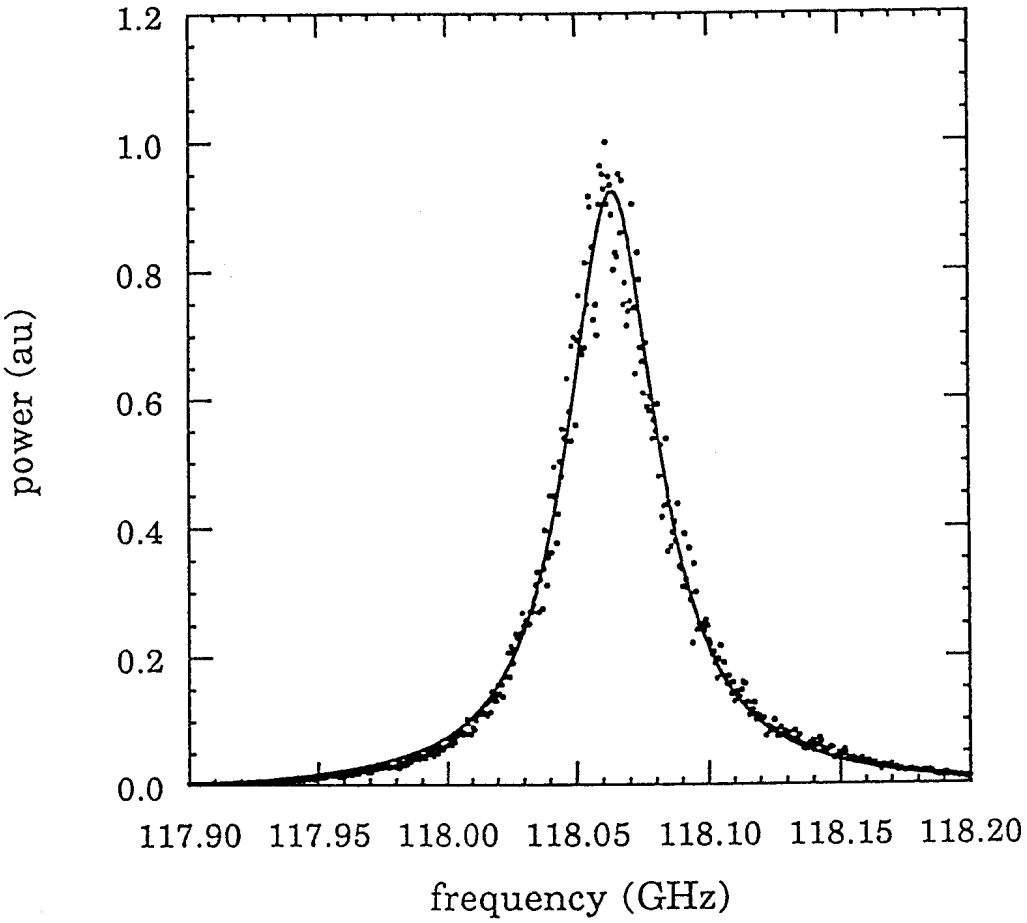

Figure 8. Resonance curve of the $TE_{22,6}$ mode in the coaxial cavity. Points - data, line - best fit to theoretical resonance curve. The best fit gives values $f_{res} = 118.06$ GHz, $Q_{tot} \sim 2800$.

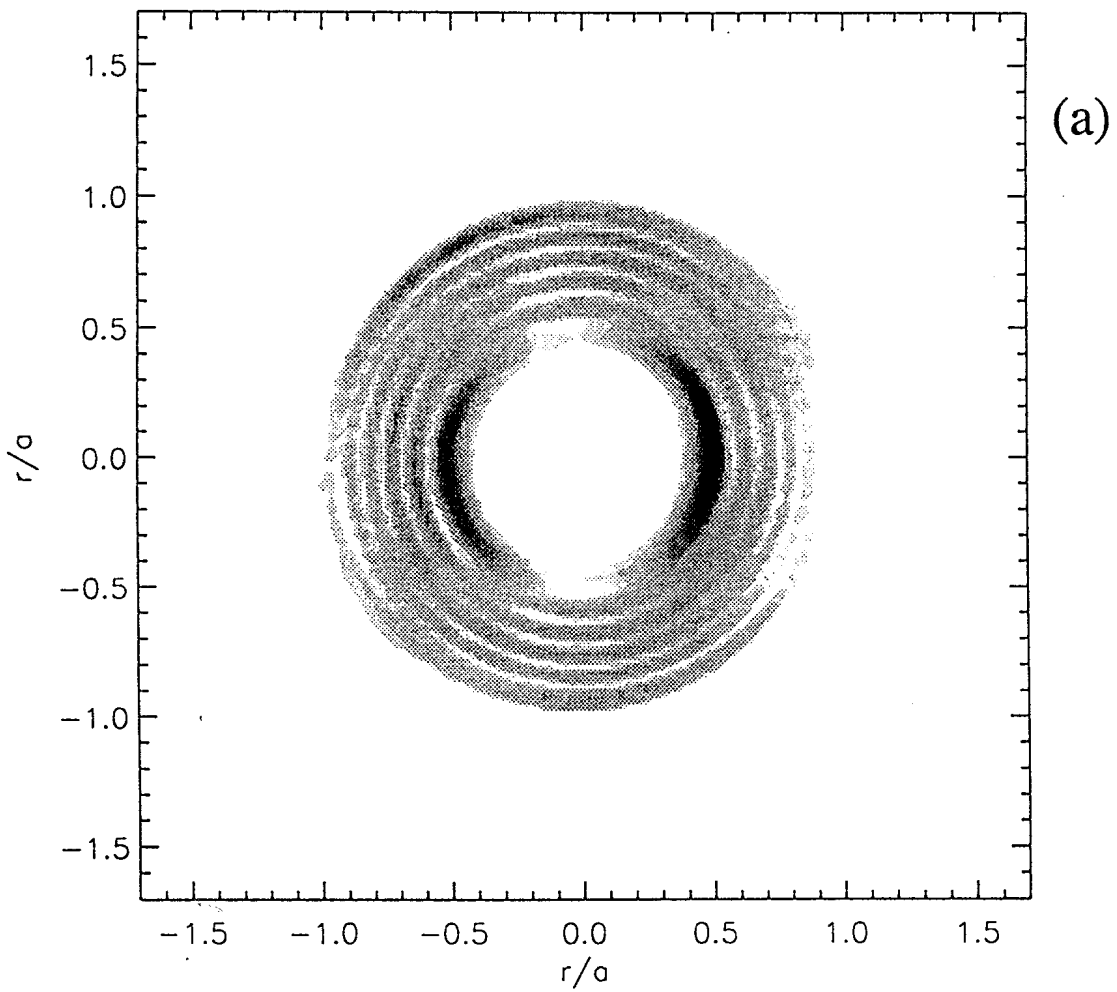

Figure 9. (a) Measured $/E_y/^2$ field distribution at output of coaxial cavity (b) Theoretical $/E_y/^2$ field distribution of the $TE_{22,6}$ mode.

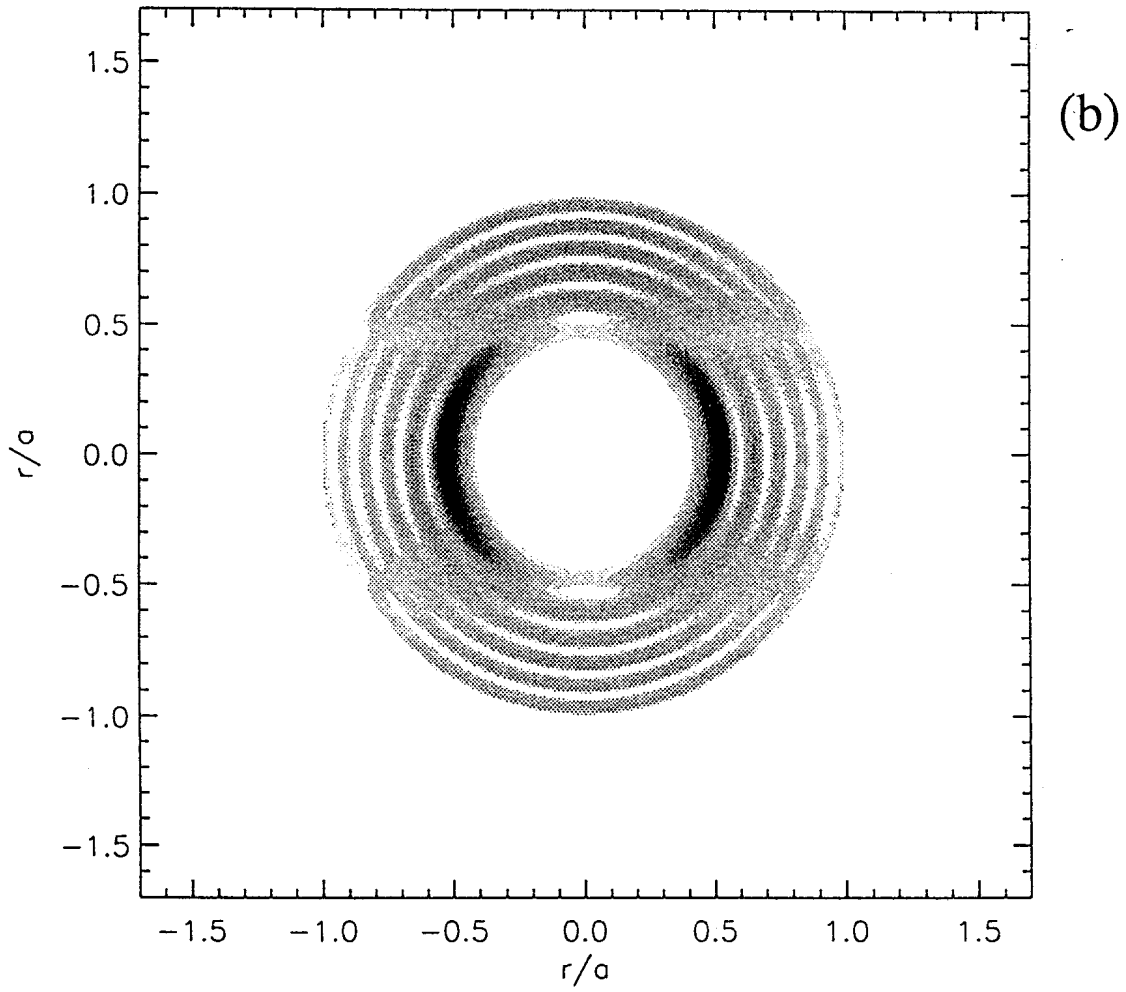

Figure 9. (a) Measured $|E_y|^2$ field distribution at output of coaxial cavity (b) Theoretical $|E_y|^2$ field distribution of the $TE_{22,6}$ mode.

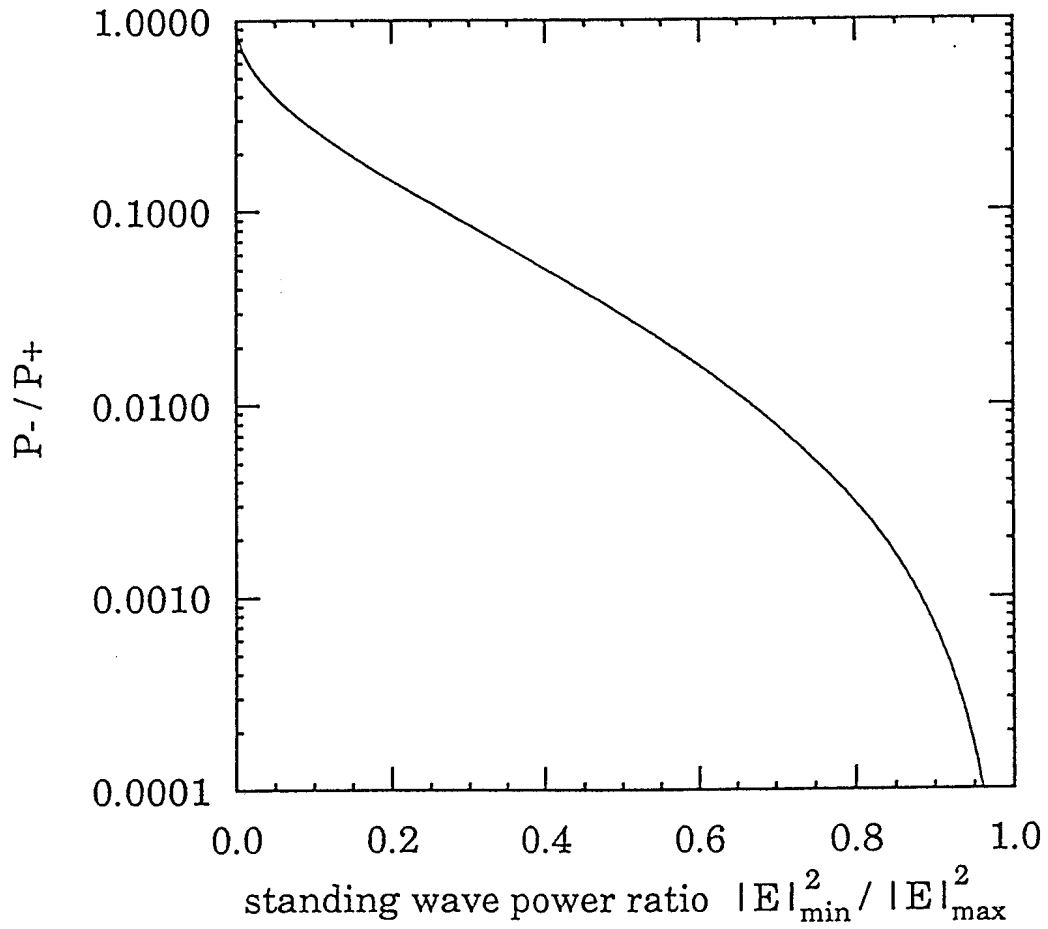

Figure 10. Counter / co-rotating mode power ratio, P^- / P^+ vs. standing wave power ratio, $/E_{min}/^2 / /E_{max}/^2$. The converter shows a standing wave ratio of *0.8* corresponding to a mode mix of $P^-_{22,6} / P^+_{22,6} \sim 0.3\%$.